

Exploring the Galaxy Mass-Metallicity Relation at $z \sim 3 - 5$

Tanmoy Laskar*, Edo Berger* and Ranga-Ram Chary†

*Harvard-Smithsonian Center for Astrophysics, 60 Garden Street, Cambridge, MA 02138

†Spitzer Science Center, California Institute of Technology, Pasadena, CA 91125

Abstract. Long-duration gamma-ray bursts (GRBs) provide a premier tool for studying high-redshift star-forming galaxies thanks to their extreme brightness and association with massive stars. Here we use GRBs to study the galaxy mass-metallicity (M_* - Z) relation at $z \sim 3 - 5$, where conventional direct metallicity measurements are extremely challenging. We use the interstellar medium metallicities of long-duration GRB hosts derived from afterglow absorption spectroscopy ($Z \approx 0.01 - 1 Z_\odot$), in conjunction with host galaxy stellar masses determined from deep *Spitzer* 3.6 μm observations of 20 GRB hosts. We detect about 1/4 of the hosts with $M_{\text{AB}}(I) \approx -21.5$ to -22.5 mag, and place a limit of $M_{\text{AB}}(I) \gtrsim -19$ mag on the remaining hosts from a stacking analysis. Using a conservative range of mass-to-light ratios for simple stellar populations (with ages of 70 Myr to ~ 2 Gyr), we infer the host stellar masses and present the galaxy mass-metallicity measurements at $z \sim 3 - 5$ ($\langle z \rangle \approx 3.5$). We find that the detected GRB hosts, with $M_* \approx 2 \times 10^{10} M_\odot$, display a wide range of metallicities, but that the mean metallicity at this mass scale, $Z \approx 0.1 Z_\odot$, is lower than measurements at $z \lesssim 3$. Combined with stacking of the non-detected hosts (with $M_* \lesssim 4 \times 10^9 M_\odot$ and $Z \lesssim 0.03 Z_\odot$), we find evidence for the existence of an M_* - Z relation at $z \sim 3.5$ and continued evolution of this relation to systematically lower metallicities from $z \sim 2$.

Keywords: gamma-ray sources (astronomical), high-redshift galaxies, cosmology

PACS: 98.62.Bj, 98.62.Ck, 98.62.Ve, 95.85.Hp, 98.52.-b, 98.58.Ay

INTRODUCTION

The simple “closed-box” model of galaxy evolution [1] predicts a correlation between the stellar mass and the gas-phase metallicity of a galaxy (the M_* - Z relation). Such a relation is indeed seen in the nearby universe [2–4], and is found to be in place out to $z \sim 2$ [5], progressively evolving to lower metallicities. Tracing the M_* - Z relation and its evolution to even earlier times will provide insight into the earliest epochs of galaxy evolution, while allowing us to probe the relative importance of various galactic-scale phenomena proposed at $z \lesssim 3$. However, studying the M_* - Z relation beyond $z \sim 3.5$ is challenging because the nebular emission lines required for robust metallicity measurements (e.g., H α , H β , N II λ 6583, O III λ 4959, 5007, O II λ 3726, 3729) shift into different near- and mid-IR wavebands, where existing spectrographs have reduced sensitivity compared to the optical band. This is aggravated by the faintness of the galaxies, making individual abundance measurements nearly impossible.

An alternative way to determine metallicities at $z \gtrsim 3$ (and in principle at $z \sim 10$ and beyond [6, 7]) is absorption spectroscopy of gamma-ray burst (GRB) optical/near-IR afterglows. Long-duration GRBs are known to be associated with the deaths of massive stars (e.g. [8]), and therefore with sites of active star formation. The large optical luminosities of GRB afterglows and their intrinsic featureless spectra provide a unique way to measure interstellar medium (ISM) metallicities for galaxies at $z \gtrsim 2$ from rest-frame ultraviolet metal absorption lines and Ly α absorption. Since the afterglows are significantly brighter than the underlying host galaxies, this technique allows us to measure metallicities independent of the galaxy brightness. This approach has now been exploited at least to $z \sim 5$ using optical spectra (e.g., [9–11]), and with near-IR spectrographs it can be implemented to $z \sim 20$.

Naturally, to explore the M_* - Z relation at $z \gtrsim 3$ we also require a determination of the GRB host galaxy stellar masses, and hence follow-up infrared observations with the *Spitzer* Space Telescope to probe the rest-frame optical luminosity. We present the first large set of *Spitzer* observations for GRB host galaxies at $z \sim 3 - 5$, and combine the inferred masses with measured metallicities to explore the M_* - Z relation beyond $z \sim 3$. A full analysis is presented in Laskar et al. (2011), to be submitted to ApJ.

GRB SAMPLE AND DATA ANALYSIS

We obtained deep observations (about 2 hr per target) of 20 long-duration GRB host galaxies in the range $z \approx 3 - 5.8$ using the $3.6 \mu\text{m}$ band of the Infra-Red Array Camera (IRAC; [12]) on-board the *Spitzer* Space Telescope. The effective wavelength of the IRAC $3.6 \mu\text{m}$ band probes the rest-frame spectral energy distribution (SED) redward of about 5500 \AA and therefore provides a robust measure of the stellar mass.

We used optical afterglow images to perform relative astrometry on the *Spitzer* mosaics and to locate the GRB hosts. At the depth of our observations, *Spitzer* images are confusion-limited for faint sources, requiring us to model and subtract nearby contaminating sources in 3 cases. We detect 5 GRB hosts at $3.6 \mu\text{m}$ (GRBs 050319, 050814, 060707, 060210, and 060926), with flux densities ranging from about 0.55 to $1.65 \mu\text{Jy}$, with a typical upper limit of about $0.25 \mu\text{Jy}$ (3σ). To assess the typical flux density of the non-detected hosts we carry out a stacking analysis of 11 non-detections with accurate relative astrometry. The stacked image does not show a detection down to a 3σ limit of $\lesssim 80 \text{ nJy}$.

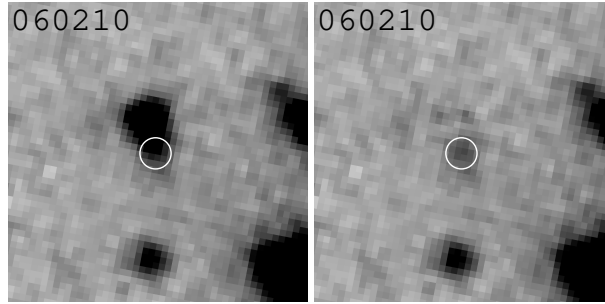


FIGURE 1. *Spitzer* $3.6 \mu\text{m}$ detection of the host galaxy of GRB 060210. Left: mosaic. Right: contaminating source subtracted. The circle ($1''$ radius) marks the afterglow position. North is up and East is to the left, while the pixels are $0''.4$ on a side.

Stellar Masses of GRB Hosts at $z \sim 3 - 5$

Computing stellar masses from observed luminosities in a given wave-band requires knowledge of the mass-to-light ratio and hence the stellar population age and metallicity. When multi-band photometry is available, modeling of the spectral energy distribution (SED) using stellar population synthesis models can be used to determine stellar masses, provided that a single stellar population is assumed. When multi-band photometry is not available, the resulting uncertainty in the mass-to-light ratio (e.g., at $\sim 1 \mu\text{m}$) is about an order of magnitude (e.g., [13]).

Here, since we lack broad-band photometry, we determine a range of mass-to-light ratios for each galaxy in the observed $3.6 \mu\text{m}$ band using a wide range of population ages and the single stellar population models of Maraston [14] with a Salpeter IMF and assuming an instantaneous burst of star formation (e-folding time, $\tau = 0$). As expected, the $3.6 \mu\text{m}$ mass-to-light ratio for these models increases with stellar population age beyond $\sim 10 \text{ Myr}$. An upper bound on the mass-to-light ratio is achieved by setting the stellar population age to the age of the universe at each host redshift ($\approx 1.8 \text{ Gyr}$ at the median redshift of our sample). We stress that this leads to a very conservative maximum mass for each host galaxy since studies of Lyman Break Galaxies (LBGs) and $\text{Ly}\alpha$ emitters (LAEs) at $z \gtrsim 3$ indicate typical population ages of $\sim 0.1 - 0.6 \text{ Gyr}$ [13, 15–17]. The median age for long-duration GRB hosts at $z \sim 1$ of about 70 Myr [18] is probably more typical. The variation in mass-to-light ratio between these age values is about an order of magnitude.

The maximal masses inferred for our sample are $(2.5 - 5.8) \times 10^{10} M_{\odot}$, while the typical (maximal) upper limits are $\lesssim 9 \times 10^9 M_{\odot}$. The masses inferred for a 70 Myr old population are about $(0.6 - 1.4) \times 10^{10} M_{\odot}$, with typical upper limits of $\lesssim 2 \times 10^9 M_{\odot}$. The mass limit from the stack of 11 GRB hosts is $\lesssim 7 \times 10^8 M_{\odot}$ for a 70 Myr old population, and $\lesssim 3 \times 10^9 M_{\odot}$ for the maximal age. We also include a literature sample of 5 long-duration GRB hosts at $z \gtrsim 3$, incorporating two detections with maximal masses of $1.4 \times 10^{10} M_{\odot}$ (GRB 060510B; [19]) and $6.7 \times 10^{11} M_{\odot}$ (GRB 080607; [20]).

THE MASS-METALLICITY RELATION AT $z \sim 3 - 5$

A typical optical afterglow spectrum exhibits a wide range of ISM absorption features due to rest-frame UV transitions of low- and high-ionization metal species, which allow a direct determination of the column density of these elements along the GRB line of sight through the host galaxy. Combined with a determination of the neutral hydrogen column density via the Ly α line, it is possible to determine the ISM abundances (e.g., [9–11]). We use S II, when available, as a measure of the metallicity, primarily since sulfur is not strongly depleted onto dust. We also place lower limits on the metallicity using Si II, Si IV and C II detections reported by Fynbo et al. [11].

Of the 18 GRBs in our sample, six have determined [S/H] values, five have no metallicity information, and six have upper limits on their metallicity from non-detections of S II as well as lower limits based on Si II or Si IV detections. For GRB 050908, the metallicity upper limit ($Z < 10^2 Z_\odot$) is not meaningful and we only report a lower limit based on a C II detection. Using these values we find a wide range of metallicities (using the Solar abundance values from Asplund et al. [21]): $Z \approx 0.01 - 1.5 Z_\odot$ for the *Spitzer*-detected GRB hosts, which have stellar masses of $\sim 2 \times 10^{10} M_\odot$. We divide the GRBs with available metallicity information (either a metallicity detection or a bounded range) into two mass bins — the $3.6 \mu\text{m}$ detections with $M_* \sim 2 \times 10^{10} M_\odot$ (Group 1) and the objects included in the stack (Group 2). For each group, we perform a Monte Carlo simulation to estimate the mean metallicity, yielding $\langle Z_1 \rangle = -1.01 \pm 0.17$ and $\langle Z_2 \rangle = -1.52 \pm 0.12$ (1σ intervals). For Group 1, the mean of the maximum inferred stellar masses is $3.7 \times 10^{10} M_\odot$, while that of the masses inferred from the 70 Myr populations is $8.8 \times 10^9 M_\odot$. To obtain mass estimates for Group 2, we scale our stack limit obtained for 11 non-detections by $\sqrt{11/7}$. Using the mean maximum mass-to-light ratio of the objects in Group 2 yields an upper limit on the mean stellar mass of these seven objects of $3.7 \times 10^9 M_\odot$, while using the mean mass-to-light ratio at 70 Myr yields a mass limit of $9.4 \times 10^8 M_\odot$.

In Figure 2, we present the absorption line metallicities plotted versus the stellar masses inferred from our *Spitzer* observations and the literature studies. The 6 GRB hosts that do not have any constraints on their ISM metallicity are excluded from this plot. We find that our two points fall below the observed relations at $z \lesssim 3.5$, providing evidence that the galaxy M_* - Z relation continues to evolve at $z \sim 3 - 5$, with our stack range probing a somewhat lower mass scale than the LBG studies at $z \sim 3.1 - 3.5$ [22, 23].

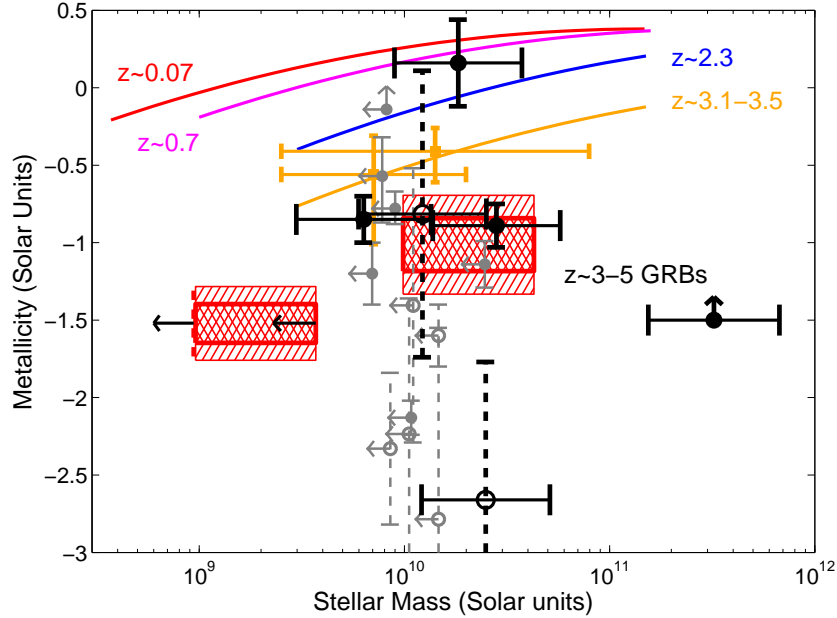


FIGURE 2. Stellar mass plotted as a function of ISM metallicity for our sample and the 5 previously observed hosts (black=detections; gray=limits). Confirmed metallicities (and one metallicity lower limit) are indicated by filled symbols, while metallicity ranges are shown by dashed vertical lines with open symbols. The hatched regions designate 1σ and 2σ intervals for estimates of the mean metallicity at two mass bins of $\sim 2 \times 10^{10} M_\odot$ ($3.6 \mu\text{m}$ detections) and $\lesssim 3.7 \times 10^9 M_\odot$ (scaled stack limit - see text). The dashed vertical line indicates the upper limit on the mean mass of the stack for a 70 Myr population. These data are consistent with a decline in metallicity with lower stellar mass — an M_* - Z relation. Also shown are the relations for $z \sim 0.07$ [3], $z \sim 0.7$ [4], $z \sim 2.3$ [5], and $z \sim 3.1 - 3.5$ [22, 23, filled squares]; the curves at $z \lesssim 2.3$ are M_* - Z relations re-calibrated by Maiolino et al. [22]. Our two points at $z \sim 3 - 5$ fall below these relations, suggesting that the M_* - Z relation continues to evolve to $z \sim 4$.

DISCUSSION AND CONCLUSIONS

We present the first study of the galaxy mass-metallicity relation at redshifts of $z \sim 3 - 5$ using GRB afterglow absorption metallicities and *Spitzer* follow-up observations. Five of the 20 GRB hosts in our sample are detected above a 3σ flux density threshold of $0.25 \mu\text{Jy}$, corresponding to a typical stellar mass of $\sim 2 \times 10^{10} M_{\odot}$. We further place a limit of $\lesssim 3 \times 10^9 M_{\odot}$ on the non-detected hosts based on a stacking analysis.

Using the metallicities of the host galaxies (inferred mainly from S II) we find a range of $\sim 10^2$ at a fixed stellar mass of $\sim 2 \times 10^{10} M_{\odot}$. The mean metallicity at this mass scale is about $0.1 Z_{\odot}$. The mean metallicity associated with 7 of the 11 the non-detected hosts, which have an upper limit of $\lesssim 3.7 \times 10^9 M_{\odot}$, is $Z \lesssim 0.03 Z_{\odot}$. Thus, there appears to be an overall decline in metallicity with decreasing mass, a hint of an M_* - Z relation. Furthermore, our two points on the M_* - Z relation lie below the relations at lower redshifts, suggesting that the relation continues to evolve at least to $z \sim 4$. Clearly, additional observations are required to confirm and increase the statistical significance of this result. A sample of 20 additional GRBs at $z \gtrsim 3$ from 2007 through the present is available for study. This will allow us to double the existing sample.

The *James Webb Space Telescope* (JWST) will provide a much deeper view of the M_* - Z relation at high redshift. For instance, the NIRCcam instrument on JWST will allow us to detect GRB hosts at $z \sim 3$ down to a mass of $\sim 10^8 M_{\odot}$, and at $z \sim 6$ to $\sim 3 \times 10^8 M_{\odot}$ with similar integration times as our observations. Equally important, the NIRSpec instrument ($1 - 5 \mu\text{m}$) will allow us to determine emission-line metallicities for some of the hosts, and hence to cross-calibrate the afterglow absorption metallicities. With on-going afterglow absorption metallicity measurements, the GRB sample will continue to play a key role in our study of high redshift galaxies.

REFERENCES

1. R. J. Talbot, Jr., and W. D. Arnett, *ApJ* **170**, 409+ (1971).
2. C. A. Tremonti, T. M. Heckman, G. Kauffmann, and others, *ApJ* **613**, 898–913 (2004), arXiv:astro-ph/0405537.
3. L. J. Kewley, and S. L. Ellison, *ApJ* **681**, 1183–1204 (2008), 0801.1849.
4. S. Savaglio, K. Glazebrook, D. Le Borgne, and others, *ApJ* **635**, 260–279 (2005), arXiv:astro-ph/0508407.
5. D. K. Erb, A. E. Shapley, M. Pettini, and others, *ApJ* **644**, 813–828 (2006), arXiv:astro-ph/0602473.
6. R. Salvaterra, M. Della Valle, S. Campana, and others, **461**, 1258–1260 (2009), 0906.1578.
7. N. R. Tanvir, D. B. Fox, A. J. Levan, and others, **461**, 1254–1257 (2009), 0906.1577.
8. S. E. Woosley, and J. S. Bloom, *ARAA* **44**, 507–556 (2006), arXiv:astro-ph/0609142.
9. E. Berger, B. E. Penprase, S. B. Cenko, and others, *ApJ* **642**, 979–988 (2006), arXiv:astro-ph/0511498.
10. J. X. Prochaska, H. Chen, M. Dessauges-Zavadsky, and others, *ApJ* **666**, 267–280 (2007), arXiv:astro-ph/0703665.
11. J. P. U. Fynbo, P. Jakobsson, J. X. Prochaska, and others, *ApJS* **185**, 526–573 (2009), 0907.3449.
12. G. G. Fazio, J. L. Hora, L. E. Allen, and others, *ApJS* **154**, 10–17 (2004), arXiv:astro-ph/0405616.
13. G. E. Magdis, D. Rigopoulou, J. Huang, and others, *MNRAS* **401**, 1521–1531 (2010), 0909.3950.
14. C. Maraston, *MNRAS* **362**, 799–825 (2005), arXiv:astro-ph/0410207.
15. A. E. Shapley, C. C. Steidel, D. K. Erb, and others, *ApJ* **626**, 698–722 (2005), arXiv:astro-ph/0503485.
16. N. A. Reddy, C. C. Steidel, D. K. Erb, and others, *ApJ* **653**, 1004–1026 (2006), arXiv:astro-ph/0609296.
17. Y. Ono, M. Ouchi, K. Shimasaku, and others, *MNRAS* **402**, 1580–1598 (2010), 0911.2544.
18. C. N. Leibler, and E. Berger, *ApJ* **725**, 1202–1214 (2010), 1009.1147.
19. R. Chary, E. Berger, and L. Cowie, *ApJ* **671**, 272–277 (2007), 0708.2440.
20. H. Chen, D. A. Perley, C. D. Wilson, and others, *ApJL* **723**, L218–L222 (2010), 1010.1002.
21. M. Asplund, N. Grevesse, and A. J. Sauval, “The Solar Chemical Composition,” in *Cosmic Abundances as Records of Stellar Evolution and Nucleosynthesis*, edited by T. G. Barnes III & F. N. Bash, 2005, vol. 336 of *Astronomical Society of the Pacific Conference Series*, pp. 25+.
22. R. Maiolino, T. Nagao, A. Grazian, and others, *A&A* **488**, 463–479 (2008), 0806.2410.
23. F. Mannucci, G. Cresci, R. Maiolino, and others, *MNRAS* **398**, 1915–1931 (2009), 0902.2398.